JOURNAL OF GEOPHYSICAL RESEARCH, VOL. 89, NO. B2, PAGES 1033–1048, FEBRUARY 10, 1984

Eruption Age of a ~100,000-Year-Old Basalt From ^{40}Ar-^{39}Ar Analysis of Partially Degassed Xenoliths

A. R. GILLESPIE,[1] J. C. HUNEKE,[2] AND G. J. WASSERBURG

The Lunatic Asylum of the Charles Arms Laboratory, Division of Geological and Planetary Sciences, California Institute of Technology

We have applied ^{40}Ar-^{39}Ar dating, using stepwise thermal extraction of Ar, to five potassium-rich granitic xenoliths and their host basalt from Sawmill Canyon in the Sierra Nevada, California. Previous K/Ar analyses showed the age of the basalt to be roughly 100,000 years or less. The xenoliths, which had accumulated large amounts of radiogenic ^{40}Ar since their crystallization ~100 m.y. ago, were partially degassed upon their inclusion in the basaltic magma. Ar released from the xenoliths in the laboratory at temperatures substantially below the melting temperature of the basalt, was created since the host magma cooled. Isotopic compositions of Ar released from the xenoliths in several extraction steps at temperatures below ~900°C were colinear in $^{36}Ar/^{40}Ar$ versus $^{39}Ar/^{40}Ar$ diagrams and defined isochrons giving a mean age of degassing of 119,000 ± 7000 (2σ) years. ^{40}Ar extracted at higher temperatures included ancient radiogenic ^{40}Ar that was never diffused from the xenoliths during immersion in the magma. This ^{40}Ar caused an increase in the apparent age for the high-temperature extractions. The high precision of the eruption age determined by this method is comparable to that obtained elsewhere by conventional K/Ar dating of sanidine. ^{40}Ar-^{39}Ar analysis of granitic xenoliths to date young basaltic lava flows may prove to yield results superior to those found from analysis of the lava itself. Establishing the age of eruption of the basalt flow in Sawmill Canyon establishes age limits for two Sierran glaciations which left moraines stratigraphically above and below the lava. Thus the younger glaciation must be Wisconsin; the older must be pre-Wisconsin in age.

1. INTRODUCTION

The purpose of this study was to demonstrate that the ^{40}Ar-^{39}Ar dating method [*Merrihue and Turner*, 1966; *Turner*, 1970, 1971*a*] with high-resolution stepwise thermal extraction of the Ar [*Jessberger et al.*, 1974] could be used to find the age of eruption of a young late Pleistocene basalt that had incorporated granitic xenoliths from a Mesozoic pluton. These xenoliths were partially degassed of their Ar upon immersion in the hot basaltic magma.

Lavas of all ages commonly contain xenoliths or xenocrysts, but especially in late Pleistocene or K-poor basalts the ^{40}Ar from incompletely degassed xenocrysts can significantly increase the apparent age of the lava. It is difficult in advance of Ar extraction to detect small xenocrysts in the samples to be dated. Previous K/Ar analyses of some young basalts [cf. *Curry*, 1971; *Bailey et al.*, 1976; *Hall and York*, 1978; *Dalrymple et al.*, 1982] have yielded inconsistent or excessive ages, perhaps due in part to such undetected xenocrysts.

Although in principal ^{40}Ar-^{39}Ar analysis should be applicable to contaminated basalts themselves [cf. *Hall and York*, 1978] we have chosen to analyze the xenoliths instead, to take advantage of their higher K content. If the xenoliths were only partially degassed by the magma, upon analysis they will contain some radiogenic ^{40}Ar (hereafter denoted by $^{40}Ar^*$) created before eruption of the lava. This residual $^{40}Ar^*$ (hereafter designated $^{40}Ar_0^*$) is expected to occupy only retentive sites and during analysis should be released only at high temperatures. New $^{40}Ar^*$ created in the xenolith after eruption will occupy all sites, including those emptied of Ar during heating in the magma. Although $^{40}Ar^*$ released at high temperatures may be dominately $^{40}Ar_0^*$, $^{40}Ar^*$ released at low temperatures (e.g., less than ~900°C) during analysis may consist entirely of new $^{40}Ar^*$. If this is the case, there should be a plateau at the age of eruption extending over the first release fractions of ^{39}Ar in the ^{40}Ar-^{39}Ar age spectrum.

Gillespie et al. [1982] have determined theoretically the circumstances for which age spectra with reasonably large plateaus at the age of eruption could be obtained from partially degassed xenoliths. Typically, for a xenolith derived from a 100-m.y.-old protolith that was immersed in magma and degassed 1 m.y. ago, more than 90% of the $^{40}Ar^*$ accumulated between crystallization and immersion must have been lost. There must also exist within the xenolith major $^{40}Ar^*$ reservoirs differing by more than a factor of ten in diffusion dimension (e.g., grain size) or a difference of roughly 15 kcal/mole in the activation energy for diffusion, so that $^{40}Ar^*$ and $^{40}Ar_0^*$ are released in different temperature ranges. Larger disparities in the ages of crystallization of the protolith and eruption of the lava require more extreme differences in parameters or more extensive degassing in the lava in order to obtain significant eruption-age plateaus. *Gillespie et al.* [1982] demonstrated that for one granitic xenolith from a Cretaceous pluton heated in a Pleistocene basaltic magma, more than 60% of the ^{39}Ar released was free of $^{40}Ar_0^*$. In the age spectrum, a plateau at 1.2 m.y. was well defined by Ar released from the xenolith in eight steps at temperatures of ~1000°C or less, even though the apparent age for subsequent steps at higher temperatures rose to 30 m.y. In a second paper, *Gillespie et al.* [1983] showed that the age of eruption given by this plateau was the same as the age of eruption found by ^{40}Ar-^{39}Ar analysis of the host basalt itself, which was rich in K (1.4% by weight) and could be readily dated.

In this paper we show that reasonable isochrons in isotope correlation diagrams and plateaus representing as much as

[1] Now at the Jet Propulsion Laboratory.
[2] Now at Charles Evans and Associates.

Paper number 3B1875.
0148-0227/84/003B-1875$05.00

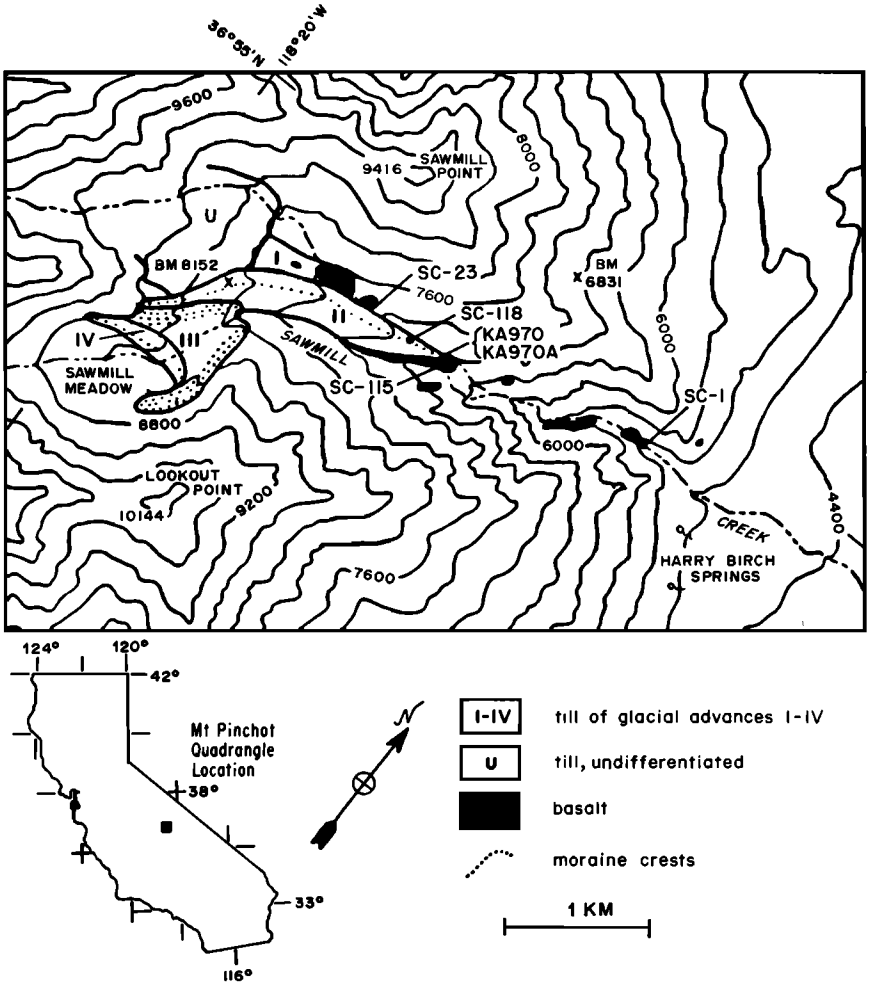

Fig. 1. Map showing sample locations in Sawmill Canyon. Glacial geology and basalt outcrops are from *Dalrymple* [1964*a*]. Samples from KA970 and KA970A were analyzed by *Dalrymple* [1964*a*]. Generalized topography with 400-ft contours is taken from the United States Geological Survey map of the Mt. Pinchot quadrangle [*York*, 1953].

50% of the ^{39}Ar in ^{40}Ar-^{39}Ar age spectra are observed for granitic xenoliths from a basalt flow an order of magnitude younger than that of *Gillespie et al.*[1983], even though the xenoliths in both lavas were from plutons of similar age. ^{40}Ar-^{39}Ar analysis of the younger samples is much more difficult because they contain about an order of magnitude less new $^{40}Ar^*$. Therefore, for a given extraction step an order of magnitude larger fractional increase in the apparent age of the younger samples will be found for the same amount of $^{40}Ar_0^*$. Consequently, it is not at all obvious a priori that enough ^{39}Ar and new $^{40}Ar^*$ can be extracted free of $^{40}Ar_0^*$ to define a plateau establishing the age of eruption.

^{40}Ar-^{39}Ar dating is preferable to conventional K/Ar dating because (1) the composition of trapped Ar (hereafter designated Ar_t) is unknown and must be assumed to calculate the K/Ar age, and (2) undetected contamination of dated samples by xenoliths or xenocrysts may increase the K/Ar age. Ideally, the ^{40}Ar-^{39}Ar technique permits determination of the Ar_t composition and recognition of the presence of $^{40}Ar_0^*$ [*Gillespie et al.*, 1982]. However, ^{40}Ar-^{39}Ar dating may introduce uncertainty because of possible recoil loss and redistribution of ^{39}Ar from grains smaller than ~30μm during neutron irradiation [cf. *Huneke and Smith*, 1976]. Basaltic lavas are especially susceptible to recoil because much of the K resides in small grains. The granitic xenoliths are themselves appropriate material for ^{40}Ar-^{39}Ar analysis, in part because the potassic grains are larger, which reduces the opportunities for recoil effects.

We chose for study a basalt flow in Sawmill Canyon in the Sierra Nevada, Inyo County, California (Figure 1). The age of the eruption was determined by *Dalrymple* [1964*a*] to be less than about 100,000 years using conventional K/Ar analyses of the host basalt, and subsequently remeasured as 53,000 ± 88,000 (2σ) years [*Dalrymple et al.*, 1982]. The basalt is contaminated by granodiorite xenoliths probably derived from the Cretaceous Spook pluton [*Moore*, 1963] through which the basalt erupted. The age of crystallization of the xenoliths is about 3 orders of magnitude greater than the age of degassing and eruption.

Sawmill Canyon cuts the eastern escarpment of the Sierra Nevada ~10 km north of Independence, California. The intercalation of basalt flows between two late Pleistocene glacial moraines in Sawmill Canyon (Figure 1) affords a valuable opportunity to obtain absolute limits on the age of Sierran glacial stages and to strengthen correlations with the better understood chronology of continental glaciation [*Dalrymple*, 1964*a*]. Basalt that issued from the north slopes of Sawmill Canyon overran an older moraine (I in Figure 1), and flowed east down the canyon to the range front. Some time later an advancing glacier deposited till (II) atop ero-

sional remnants of this flow. Thus a date on this interglacial basalt flow provides a lower limit for glacial advance I and an upper limit for glacial advance II.

2. SAMPLE SITES

We sampled the basalt at several locations in Sawmill Canyon (Figure 1). SC-1 is near the range-front fault. SC-23 is ~10 m north of the contact between moraine II and the eastern of the two basalt remnants on the north side of Sawmill Canyon. SC-115 and SC-118 underlie moraine II. Site SC-115 is on the same outcrop from which *Dalrymple* [1964*a*] obtained his basalt samples KA970 and KA970A (Figure 1). From the geologic relationships it is probable that the lava flow at SC-1 is older than moraine II. At each location samples were chosen that contained xenoliths. By analyzing a number of xenoliths from different positions in the flow, we hoped to increase the chances of finding one degassed sufficiently to yield an eruption age.

3. PETROGRAPHY

The lava at site SC-1 is a fresh appearing non-vesicular olivine basalt that contains abundant clinopyroxene and plagioclase phenocrysts in a matrix of smaller (~100 μm) plagioclase laths and pyroxene crystals. K probably resides primarily in very small crystals and glass blebs (~10 μm) in the groundmass. Electron microprobe analysis showed one glass bleb to have the composition of leucite. *Dalrymple* [1964*a*] determined that K from the host basalt near SC-115 constituted 1.4% of the rock by weight. Granodiorite xenoliths and isolated xenocrysts derived therefrom are encountered in the basalt. Basalt samples 2-2 and 2-3 from SC-1 were taken more than 20 cm from the nearest observed xenoliths. Thin sections revealed no sign of devitrification or other alteration of the lava.

Grandiorite xenoliths were collected from each of the four sites (SC-1, 23, 115, and 118). The xenoliths were probably derived from the Spook pluton [*Moore*, 1963], through which the host basalt erupted. The granodiorite of the Spook pluton is composed of approximately 24% quartz, 19% K-feldspar, 48% plagioclase, 6% biotite, and lesser amounts of hornblende and accessory minerals [*Moore*, 1963]. The K-feldspar is generally perthitic, with lamellae about 50 μm in width. Some grains exhibit microcline twinning. The Spook pluton is porphyritic, with K-feldspar phenocrysts as much as 2 cm in length. Both plagioclase and, to a lesser extent, K-feldspar grains generally contain turbid zones of mafic inclusions [*Moore*, 1963] and alteration products. Plagioclase grains contain small crystals of eipdote. Feldspar grains in the xenoliths have a similar appearance.

Dalrymple [1964*a*] observed that some of the perthitic K-feldspar in the xenoliths had been altered to sodic sanidine. This alteration was probably due to heating by the magma. The edges of the xenoliths are corroded by reaction with the basaltic magma. Some may be easily crumbled with a hammer, but in thin section even these xenoliths do not appear markedly more altered than samples of the Spook pluton taken far from the lava flow. Most of the xenoliths are small, but some as large as 15 cm in diameter have been found.

At site SC-1, two granodiorite xenolith less than 5 mm in diameter were acquired (sample 6-8; and samples 6-17, 9-1, and 9-2). These xenoliths were not easily disaggregated. At site SC-23, five samples (6-16, 6-25, 9-4, 9-5, and 9-6) were taken from a single 20-cm xenolith. One of these, sample 6-16, was part of a 2-cm K-feldspar phenocryst. The others were whole pieces of the xenolith and contained several mineral phases. The surface of the xenolith was pitted where feldspar grains in contact with the basaltic magma had been melted. Similar xenoliths were also collected at sites SC-115 and SC-118. The K-feldspar phenocryst (sample 6-16) consisted of 3-mm grains in optical continuity. There were numerous inclusions of albite and fewer inclusions of accessory minerals such as sphene. Alteration products were less abundant than in the rest of the xenolith. Faint and diffuse perthitic zones indicate that some annealing occurred, probably during heating in the magma. The grains were fractured at intervals of about 300 μm. No microcline twinning was observed. X ray diffraction analysis showed the presence of orthoclase and albite.

4. ANALYTIC TECHNIQUES

4.1. *Sample Preparation*

Basalt samples weighing ~0.5 g were picked from the interior of a block from SC-1 after coarse crushing. Samples were visually checked for xenocrysts, and none were found on exposed surfaces. The basalt samples were wrapped in Al foil packets for neutron irradiation. Xenolith samples were treated in different ways. Samples 6-16, 6-25, 9-4, and 9-5 from SC-23 were irradiated in foil and then unwrapped before analysis to reduce the amount of nonradiogenic Ar. Sample 9-6 (also from SC-23) was gently crushed and etched in 20% HF at 25°C for 100 s. This was done to remove any fine-grained alteration products from the surface of grains. Sample 9-6 was the only sample so treated. Feldspars larger than ~0.5 mm were then hand-picked from the etched material and wrapped in Sn foil. Sn foil was used because it melts at a lower temperature (232°C) than Al (660°C), and thus contributed to the Ar blank only during the first extraction step (275°–500°C). Xenolith samples from SC-115, SC-118, and SC-1 were gently crushed and sieved. Felsic grains from the size fraction 104–160 μm were separated magnetically and wrapped in foil for neutron irradiation. The intent was to simplify the mineralogy by excluding biotite, hornblende, and any fragments of basalt.

Samples were enclosed along with Bern 4M standard muscovite [*Jäger et al.*, 1963], CaF_2, and Ni wire irradiation monitors in evacuated quartz capsules for neutron irradiation, as described in *Gillespie et al.* [1982]. The ^{40}Ar-^{39}Ar age of the muscovite standard was taken as 17.86 ± 0.62 (2σ) m.y. [*Dalrymple and Lanphere*, 1971]. This age was corrected for the new ^{40}K abundance and decay constant $\lambda \equiv \lambda_e + \lambda_\beta = 5.543 \times 10^{-10}\ y^{-1}$ recommended by *Steiger and Jäger* [1977]. Samples were irradiated with fast neutrons for 30 min or 60 min (~10^{17} n cm^{-2}) in the central thimble of the TRIGA reactor facility of the United States Geological Survey at Denver, Colorado [*Dalrymple et al.*, 1981].

4.2. *Analysis of Ar*

Details of Ar extraction and analysis were similar to those of *Gillespie et al.* [1983] and *Radicati di Brozolo et al.* [1981], except for minor differences in mass discrimination and sensitivity factors [*Gillespie*, 1982]. Most of the Ar used to determine isochrons was extracted at temperatures less than ~1000°C. Blank levels of ^{40}Ar at these temperatures generally ranged from 2.6×10^{-9} to 3.5×10^{-8} cm^3 STP (for two

TABLE 1. Results of ^{40}Ar-^{39}Ar Analyses of Neutron-Irradiated Basalt and Granitic Xenoliths From Sawmill Canyon, Sierra Nevada, Inyo County, California

Sample	Site	Type	Sample Mass, mg	^{40}Ar, cm^3 STP/g $\times 10^8$	$^{36}Ar/^{40}Ar$ $\times 10^5$	$^{39}Ar/^{40}Ar$† $\times 10^4$	Age Proportionality Factor $\times 10^4$	K Weight, %	Ca Weight, %	Total Age, m.y.
2-2	SC-1	basalt	533	21	320 ± 5	831 ± 7	2.382	1.4	12.2	0.28 ± 0.07
2-3	SC-1	basalt	411	16	322 ± 6	829 ± 19	2.382	1.2	11.4	0.25 ± 0.08
6-8	SC-1a	xenolith	422	208	276 ± 51	121 ± 2	1.196	4.0	2.9	3.3 ± 0.1
6-17	SC-1b	xenolith	228	90	291 ± 7	331 ± 5	1.196	4.7	2.1	0.9 ± 0.1
9-4	SC-1b	xenolith	105	229	304 ± 82	156 ± 7	1.167	5.5	7.2	1.4 ± 0.4
9-5	SC-1b	xenolith	111	211	301 ± 3	167 ± 1	1.167	5.4	2.4	1.4 ± 0.2
6-16	SC-23	feldspar	361	200	130 ± 3	264 ± 4	1.196	7.1	0.7	5.1 ± 0.3
6-25	SC-23	xenolith	343	129	233 ± 41	184 ± 1	1.196	3.8	2.8	3.7 ± 0.2
9-1	SC-23	xenolith	222	59	245 ± 3	225 ± 1	1.167	4.6	2.0	2.6 ± 0.3
9-2	SC-23	xenolith	275	148	215 ± 74	181 ± 4	1.167	4.4	8.4	4.3 ± 0.3
9-6	SC-23	microcline	340	1050	20 ± 1	31 ± 0	1.167	5.2	3.4	64.8 ± 0.7
7-82	SC-115	xenolith	442	50	101 ± 7	193 ± 2	1.020	3.4	1.5	6.8 ± 0.2
7-63‡	SC-118	xenolith	330	>86	232 ± 24	104 ± 1	1.020	>2.4	>1.5	5.7 ± 0.4

Column 5 shows the amount of ^{40}Ar extracted from each sample normalized by the sample mass, and corrected for system blank. Next columns show the composition, after correction for interference isotopes and system blank (uncertainties are 2σ). Apparent total age (last column) is found from these compositons, utilizing a proportionality factor found from the $^{39}Ar/^{40}Ar^*$ of the Bern 4 M irradiation monitor and assuming and Ar_t of atmospheric composition. Ages are found according to $\lambda^{-1} \ln \{a[(^{36}Ar/^{40}Ar)_t - (^{36}Ar/^{40}Ar)_{sample}]/[(^{36}Ar/^{40}Ar)_t (^{39}Ar/^{40}Ar)_{sample}] + 1\}$ where a is the proportionality factor listed in the table. Concentrations of K and Ca were calculated from ^{39}Ar and ^{37}Ar compared to abundance of the same isotopes in the Bern 4M and $CaCO_3$ irradiation monitors of known K and Ca.

†Normalized to neutron fluence for muscovite irradiation monitor.

‡Step lost in analysis.

analyses, 9-1 and 9-2, the blank was much higher: 2×10^{-7} cm^3 STP).

The isotopic composition of the blank Ar was measured repeatedly. The crucible was degassed at ~1750°C for several hours between each sample to reduce memory. We found that after several samples had been run the composition of the blank Ar had become somewhat enriched in ^{40}Ar, typically to values of $^{36}Ar/^{40}Ar \approx 0.0032$. Blank Ar was subtracted according to compositions measured in sequences of three to eight extractions run at various temperatures both before and after analysis of each sample.

Because of the desire to measure at least four increments of Ar free of $^{40}Ar_0^*$, small temperature increments between low-temperature steps were used. Sample sizes were limited to ~1 g by the extraction line, which resulted in blank Ar comprising a large fraction of the measured Ar in some steps (especially for the basalt samples). Blank Ar was the major source of uncertainty in these steps.

4.3. *Presentation of Ar Analyses*

Ar data are presented primarily as composition variation trajectories in plots of $^{36}Ar/^{40}Ar$ versus $^{39}Ar/^{40}Ar$. The trajectories describe the changing composition of Ar as the extraction temperature is raised. In general, Ar compositions will range between two endmembers: a trapped component on the $^{36}Ar/^{40}Ar$ axis, and a K-derived component on the $^{39}Ar/^{40}Ar$ axis. For partially degassed granitic xenoliths, the Ar compositions of the first extractions tend to plot in a linear array until the extraction temperature exceeds some level, often ~900–1000°C [*Gillespie et al.*, 1983], and from this array an isochron may be determined. The intercept of the isochron with the $^{36}Ar/^{40}Ar$ axis is a measure of the composition of Ar_t in the mineral phases releasing Ar below these temperatures. The intercept with the $^{39}Ar/^{40}Ar$ axis corresponds to the ratio of K-derived ^{39}Ar to new $^{40}Ar^*$ created since degassing of the xenolith in the lava. The K-derived $^{39}Ar/^{40}Ar^*$ is inversely proportinal to $[\exp(\lambda t) - 1]$, where t is the age, but for Quaternary events $^{39}Ar/^{40}Ar^*$ is inversely proportional to t with less than 0.05% error. The proportionality factors are listed in Table 1. Samples in this study were neutron-irradiated in several different batches, so the factors differ from sample to sample. Consequently, we have standardized the abscissa of the three-isotope diagrams to the equivalent units of reciprocal age. Only if $^{36}Ar/^{40}Ar = 0$ does the measured $^{39}Ar/^{40}Ar$ actually specify an age.

The isochrons in the three-isotope diagrams were determined by linear regression of those consecutive low-temperature Ar compositions that appeared to be colinear. The method of *Williamson* [1968], which accommodates compositions of different uncertainties, was used if measurement errors seemed to be the only source of uncertainty. Otherwise, regression to the reduced major axis [*Kermack and Haldane*, 1950] was used. The reduced major axis is the best regression line if condition *c* of *York* [1966, p. 1083] is fulfilled. In every analysis the first step for which $^{40}Ar_0^*$ was significant had to be determined. If compositions affected by $^{40}Ar_0^*$ were inadvertently used to define a regression line, then this line would provide upper limits to the age of eruption and to $(^{36}Ar/^{40}Ar)_t$.

We have used age spectra in this study to exhibit the fraction of ^{39}Ar released before $^{40}Ar_0^*$ was detected. This information is not evident in the three-isotope diagrams. Apparent ages were calculated at each step from the K-derived $^{39}Ar/^{40}Ar^*$, found by subtracting $^{40}Ar_t$ in proportion to ^{36}Ar from the measured ^{40}Ar. It was assumed that there was a single Ar_t for which the composition was given by the $^{36}Ar/^{40}Ar$ axis intercept of the isochron defined above. For the extremely young eruptions dated in this study, violation of these assumptions would probably result in distorted or unrecognizable plateaus at the age of eruption [cf. *Huneke*, 1976; *Lanphere and Dalrymple*, 1976]. The age spectra will be accurate if there was indeed a single Ar_t of the calculated composition, or if the amount of $^{40}Ar^*$ greatly exceeded the amount of $^{40}Ar_t$. Our approach differs from the usual method in that the composition of Ar_t was not taken to be precisely atmospheric, but was determined for each sample analyzed.

TABLE 2. Isochron Characteristics for ^{40}Ar-^{39}Ar Analyses of Neutron-Irradiated Granitic Xenoliths From Sawmill Canyon

Sample	Site	Number of Steps Free of $^{40}Ar_0$*	Fraction of ^{39}Ar in Steps Free of $^{40}Ar_0$*	$(^{36}Ar/^{40}Ar)_t \times 10^5$	Isochron Age, years
6-8	SC-1a	8	0.47	332 ± 4	119,000 ± 8,000
6-17	SC-1b	4	0.54	334 ± 4	122,000 ± 22,000
9-4	SC-1b	3	0.52	335 ± 5	84,000 ± 28,000
9-5	SC-1b	4	0.56	336 ± 2	115,000 ± 24,000
(mean†)	SC-1	...	...	...	117,000 ± 7,000
6-16	SC-23	5	0.19	325 ± 7	161,000 ± 24,000
6-25	SC-23	8	0.55	333 ± 3	117,000 ± 11,000
9-1	SC-23	5	0.53	337 ± 7	125,000 ± 23,000
9-2	SC-23	4	0.53	334 ± 9	104,000 ± 37,000
(mean†)	SC-23	...	...	...	123,000 ± 9,000
(mean†)	SC-1, 23	...	...	...	119,000 ± 5,000

Lines in the $^{36}Ar/^{40}Ar$ versus $^{39}Ar/^{40}Ar$ diagram fit to Ar compositions thought to be free of $^{40}Ar_0$* and thought to be mixtures of a single Ar_t and a single K-derived component were interpreted as isochrons. The composition of Ar_t (column 5) was specified by the intersection of the isochron and the $^{36}Ar/^{40}Ar$ axis. The isochron age (last column) was calculated from the intersection of the isochron and the $^{39}Ar/^{40}Ar$ axis. This age does not assume an Ar_t of atmospheric composition. Ar compositions for individual steps are given in Table 3.

†Mean age for isochrons for all samples (ages weighted by variance).

(For samples that showed correlated isotopic systematics, we also compounded the uncertainty in the determination of the Ar_t composition in calculating the uncertainty of the apparent age.)

5. RESULTS

In Table 1 are found amounts of ^{40}Ar and ^{36}Ar released from each sample, and the corresponding compositions $^{36}Ar/^{40}Ar$ and $^{39}Ar/^{40}Ar$. From these compositions, model total ages are calculated assuming $(^{36}Ar/^{40}Ar)_t = 0.003384$ (atmospheric Ar). Total ages for the xenoliths reflect the extent of degassing in the magma, but cannot be used to determine the actual age of degassing. Abundances of K and Ca inferred from $^{39}Ar_K$ and $^{37}Ar_{Ca}$ are also reported in Table 1. Information pertaining to isochrons and inferred ages of degassing or eruption is given in Table 1. Unlike the total ages from Table 1, these ages do not depend on an assumed atmospheric Ar_t. For samples not listed in Table 2, reasonable isochrons were not observed.

Table 3 gives summary Ar compositions for each incremental extraction from each sample. Complete composition data may be found in the work of *Gillespie* [1982]. Model ages are also given in Table 3 for each incremental extraction of Ar from the samples. We assumed an atmospheric Ar_t in order to calculate these ages. This was necessary because in general the actual Ar_t cannot be determined for individual Ar extractions, but must be found by extrapolating trends in Ar compositions determined for several steps, as was done for Table 2. We do not infer actual ages of eruption from the apparent ages given in Table 3. These apparent ages are useful primarily in identifying those extractions that included $^{40}Ar_0$*.

Uncertainties given in the discussion and tables are 2σ; error bars in the figures are 1σ, except as noted.

5.1. *Samples from Site SC-1*

Two samples of basalt and four samples of granitic xenoliths from the lava flow at the mouth of Sawmill Canyon (SC-1) were analyzed. Abundances of K and Ca inferred for the basalt were ~1.3% and ~11.8% by weight, respectively; average values of 4.5% and 3.5% were found for the xenoliths.

Basalt samples. Three-isotope diagrams for basalt samples 2-3 and 2-2 are shown in Figure 2. Ar from 2-3 was extracted in nine steps at temperatures from ~275°C to ~1375°C (Table 3*a*). The total age was 250,000 ± 80,000 years. Low-temperature steps were dominated by Ar_t. ^{40}Ar extracted at ~675°C was largely radiogenic, but the uncertainty in the composition was larger than for other steps because the amount of Ar released was so small. Upon fusion the Ar released from the basalt was once again primarily Ar_t. Thus with increasing temperatures, Ar compositions progressed from near "AIR" to a radiogenic composition and returned to "AIR." This was the general pattern observed by *Gillespie et al.* [1982] for basalts from the nearby North Fork of Oak Creek, and by *Hall and York* [1978] for late Pleistocene basalts from France. However, the compositions for 2-3 were not colinear, and no isochron could be established. Instead, Ar from the first four steps appeared to lie on one line, indicating an apparent age of ~0.5 m.y., while subsequent compositions defined different trends and yielded younger ages. While there is no straightforward interpretation, the composition trajectory does not seem to have been affected by $^{40}Ar_0$* at high temperatures. Thus the composition trajectory showed neither simple binary mixing, as expected for basalt with a single trapped component, nor the complicated pattern found for partially degassed xenoliths by *Gillespie et al.* [1983].

The second basalt sample (2-2) yielded a total age of 280,000 ± 70,000 years, similar to the age for basalt 2-3. The composition trajectory for 2-2 did not appear to define an isochron, and the most radiogenic step (650°C) plotted below the trend established by the four other compositions. The fusion step (~1400°C) plotted near the ordinate but distinctly below "AIR," possibly indicating the presence of excess ^{40}Ar, either from $^{40}Ar_0$* or from a ^{40}Ar-rich Ar_t. If this is true, then the total ages, calculated assuming an atmospheric Ar_t, are too high.

TABLE 3*a*. Stepwise Summary of ^{40}Ar-^{39}Ar Analyses of Neutron-Irradiated Basalt and Granitic Xenoliths From Sawmill-Canyon: Basalt From Site SC-1

T, °C	^{40}Ar cm^3 STP g^{-1} × 10^8	^{40} Ar(Blank) cm^3 STP g^{-1} × 10^8	^{39}Ar/^{40}Ar × 10^4	^{36}Ar/^{40}Ar × 10^5	F_{39}	Model Age, m.y.
			Sample 2-3			
275	2.6	0.06	467 ± 3	321 ± 8	0.09	0.47 ± 0.22
300	1.5	0.08	651 ± 7	315 ± 4	0.17	0.47 ± 0.08
375	0.47	0.08	853 ± 17	311 ± 16	0.19	0.41 ± 0.24
425	0.40	0.08	1525 ± 14	278 ± 40	0.23	0.51 ± 0.34
500	0.16	0.09	7201 ± 42	228 ± 209	0.27	0.20 ± 0.37
675	0.22	0.10	22925 ± 2294	51 ± 127	0.48	0.16 ± 0.14
850	0.33	0.12	9801 ± 43	237 ± 40	0.64	0.13 ± 0.05
1000	0.55	0.15	3893 ± 25	301 ± 20	0.76	0.12 ± 0.06
1375[f]	13.	3.1	305 ± 1	332 ± 7	1.00	0.28 ± 0.29
			Sample 2-2			
500	5.5	0.05	1736 ± 9	318 ± 5	0.56	0.15 ± 0.04
650	0.29	0.05	6979 ± 22	258 ± 30	0.66	0.15 ± 0.05
800	0.37	0.05	3574 ± 30	311 ± 12	0.72	0.10 ± 0.05
1000	1.0	0.06	857 ± 1	323 ± 3	0.77	0.27 ± 0.05
1400[f]	14.	0.87	285 ± 1	322 ± 7	1.00	0.72 ± 0.31

[f]Denotes step in which fusion occurred.

In both basalt analyses Ar extracted at temperatures around 650°C was dominated by the system blank (Table 2). This dominance would have been reduced had we used larger samples; however, it is unlikely that this change would have yielded isochrons for either analysis. Blank correction shifts compositions away from the ^{36}Ar/^{40}Ar axis along lines connecting the blank and the measured compositions. One consequence is that blank correction usually does not strongly affect apparent ages or disturb trends in the isotopic variation trajectories, unless blank Ar and Ar$_r$ are very different in composition. In sample 2-3, even steps for which blank Ar was not important failed to define an isochron. In sample 2-2, no reasonable blank correction (diagonal error bar in Figure 2) could have forced the deviant 650°C step onto the line defined by the other compositions.

Xenolith samples. Trajectories of Ar compositions for the four samples of granitic xenoliths from the same site as the basalt samples (SC-1) were distinctly different from those for the basalts, and resembled those predicted by *Gillespie et al.* [1982] for partially degassed samples and those measured by *Gillespie et al.* [1983] for xenoliths from a 1-m.y.-old lava flow. Data are summarized by step in Table 3*b* and three-isotope diagrams are shown in Figure 3. In general, compositions progressed, with increasing extraction temperature, from a point near "AIR" on the ordinate and along lines that intersected the abscissa at ^{39}Ar/^{40}Ar compositions corre-

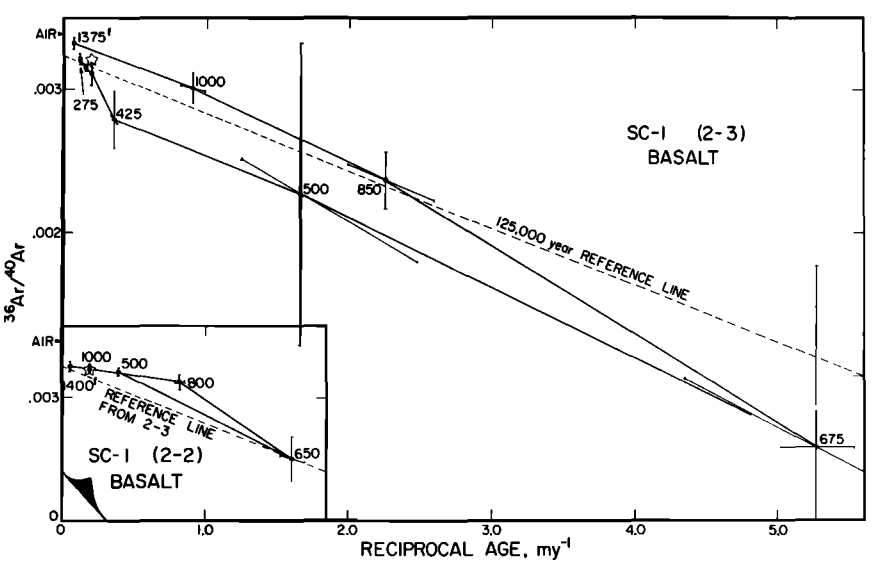

Fig. 2. Three-isotope diagrams of ^{36}Ar/^{40}Ar versus ^{39}Ar/^{40}Ar for basalt analyses. The abscissa gives ^{39}Ar/^{40}Ar values normalized to units of reciprocal age. Compositions of Ar mixed from a single trapped Ar and a single K-derived Ar will plot on a line that defines an isochron and from which the end-member compositions may be inferred. Ar compositions for the basalt samples were not colinear and could not be used to determine reliable isochrons. The total composition of Ar released in all steps, shown by the star symbol, gave a model age of ~270,000 years. A 125,000-year line (fit to the Ar compositions for sample 2-3) is shown in both diagrams for reference. Error bars in these and subsequent three-isotope diagrams are 1σ. Diagonal error bars reflect uncertainties in blank subtraction. Extraction temperatures (°C) are shown for selected steps. Superscript *f* identifies the step in which fusion occurred.

TABLE 3*b*. Granodiorite Xenoliths From Site SC-1

T, °C	^{40}Ar cm^3 STP g^{-1} × 10^8	^{40} Ar(Blank) cm^3 STP g^{-1} × 10^8	^{39}Ar/^{40}Ar × 10^4	^{36}Ar/^{40}Ar × 10^5	F_{39}	Model Age, m.y.
			Sample 6-8 (SC-1a)			
275*	7.6	0.11	15 ± 0	333 ± 1	0.004	2.4 ± 0.4
300*	2.5	0.14	81 ± 0	329 ± 1	0.01	0.7 ± 0.1
400*	1.1	0.14	83 ± 1	328 ± 8	0.02	0.2 ± 0.2
400*	4.2	0.14	39 ± 0	330 ± 1	0.03	1.4 ± 0.2
500*	1.3	0.14	1400 ± 15	313 ± 2	0.09	0.115 ± 0.009
675*	1.3	0.14	2624 ± 4	278 ± 3	0.22	0.146 ± 0.008
775*	0.68	0.14	5797 ± 34	227 ± 5	0.34	0.124 ± 0.005
875*	0.73	0.14	5657 ± 26	233 ± 4	0.47	0.120 ± 0.005
950	0.87	0.14	3928 ± 28	245 ± 6	0.59	0.151 ± 0.010
1025	0.58	0.14	2499 ± 9	270 ± 5	0.63	0.175 ± 0.014
1100	1.3	0.14	971 ± 1	281 ± 3	0.67	0.38 ± 0.02
1200	4.9	0.14	277 ± 1	295 ± 1	0.73	1.02 ± 0.02
1700	180.	4.5	39 ± 0	271 ± 1	0.99	11.3 ± 0.2
1700	11.	4.5	20 ± 2	260 ± 19	1.00	24.9 ± 6.2
			Sample 6-17 (SC-1b)			
300*	1.8	0.22	243 ± 3	334 ± 3	0.01	0.13 ± 0.09
500*	7.1	0.27	481 ± 2	324 ± 1	0.12	0.20 ± 0.02
675*	5.8	0.27	832 ± 5	317 ± 2	0.29	0.16 ± 0.02
775*	3.8	0.33	2137 ± 7	294 ± 2	0.54	0.13 ± 0.01
950	4.6	0.33	1450 ± 2	298 ± 2	0.75	0.18 ± 0.01
1100	4.7	0.33	627 ± 2	299 ± 3	0.84	0.40 ± 0.03
1400	42.	2.3	113 ± 1	260 ± 5	0.99	4.5 ± 0.3
1750	51.	27.	9 ± 1	319 ± 17	1.00	14.6 ± 12.6
			Sample 9-4 (SC-1b)			
300*	37.	2.3	6 ± 0	336 ± 2	0.01	2.8 ± 1.8
500*	22.	2.3	458 ± 26	329 ± 33	0.28	0.13 ± 0.45
600*	6.9	2.3	1740 ± 14	313 ± 6	0.52	0.09 ± 0.02
725	7.3	2.3	990 ± 198	307 ± 8	0.67	0.20 ± 0.06
825	19.	2.3	295 ± 1	294 ± 2	0.82	0.95 ± 0.05
950	48.	2.3	101 ± 1	255 ± 2	0.96	5.2 ± 0.1
1400	34.	18.	68 ± 2	244 ± 5	0.99	8.8 ± 0.5
1750	150.	76.	9 ± 11	327 ± 19	1.00	· · ·
			Sample 9-5 (SC-1b)			
275*	57.	2.4	2 ± 0	337 ± 1	0.004	5.5 ± 4.3
350*	24.	2.4	18 ± 0	334 ± 2	0.02	1.7 ± 0.6
475*	11.	2.4	508 ± 2	326 ± 3	0.15	0.15 ± 0.04
600*	11.	2.4	1533 ± 3	308 ± 4	0.56	0.12 ± 0.02
725	16.	2.4	573 ± 2	271 ± 2	0.79	0.75 ± 0.02
900	28.	2.4	166 ± 1	247 ± 2	0.92	3.5 ± 0.1
1400	47.	10.	69 ± 1	257 ± 4	1.00	7.4 ± 0.4
1750	100.	72.	0 ± 4	317 ± 16	1.00	· · ·

*Steps used to find isochrons.

sponding to ages of 84,000–122,000 years. Above temperatures of 600°–875°C compositions were increasingly enriched in ^{40}Ar, so that at the highest temperature steps they fell once again near the ordinate, but well below "AIR." This pattern was interpreted by *Gillespie et al.* [1983] to indicate that the release of Ar created or introduced into the sample after degassing in the magma was augmented at high temperatures by $^{40}Ar_0$*. Sufficient amounts of $^{40}Ar_0$* were released to yield maximum ages of 25 m.y. and total ages of 0.9–3.3 m.y., well above the age of ~100,000 years indicated by the Ar released at low temperatures.

The analysis of xenolith sample 6-8 (site SC-la) was exceptional in that the first eight steps gave colinear compositions indicating mixing between a single Ar_t and a well-defined K-derived Ar (Figure 3). The line fit to these eight compositions indicated $(^{36}Ar/^{40}Ar)_t$ = 0.00332 ± 0.00004, distinctly richer in ^{40}Ar than atmospheric Ar, and an age of 119,000 ± 8000 years. The high precision of the age resulted from the large number of steps and from the large radiogenic component (~33%) of the ^{40}Ar released in the 775°C and 875°C steps. Half the total ^{39}Ar was released in the first eight steps. At higher temperatures Ar compositions fell on a line passing through $^{36}Ar/^{40}Ar \approx 0.003$. According to the interpretive model of *Gillespie et al.* [1982], this trend resulted largely from increasing amounts of $^{40}Ar_0$* extracted from previously undepleted reservoirs. In this scheme, the observed linearity of the compositions from 775°C to 1200°C would be spurious. Ar extracted at 1700°C was significantly enriched in ^{40}Ar and plotted on the ordinate well below other compositions.

^{40}Ar-^{39}Ar analyses of the three samples of the second granitic xenolith, SC-1b, differed from that of 6-8 mainly in that fewer steps were free of $^{40}Ar_0$*. For no step free of $^{40}Ar_0$* was ^{40}Ar more than 13% radiogenic. The total ages were less than half that for 6-8, and hence degassing in the lava may have been more complete; despite this, $^{40}Ar_0$* was detected at temperatures as low as ~725°C in two of the samples (9-4 and 9-5). This was 225°C lower than for 6-8. In each of the samples more than half of the total ^{39}Ar was released before $^{40}Ar_0$* was detected.

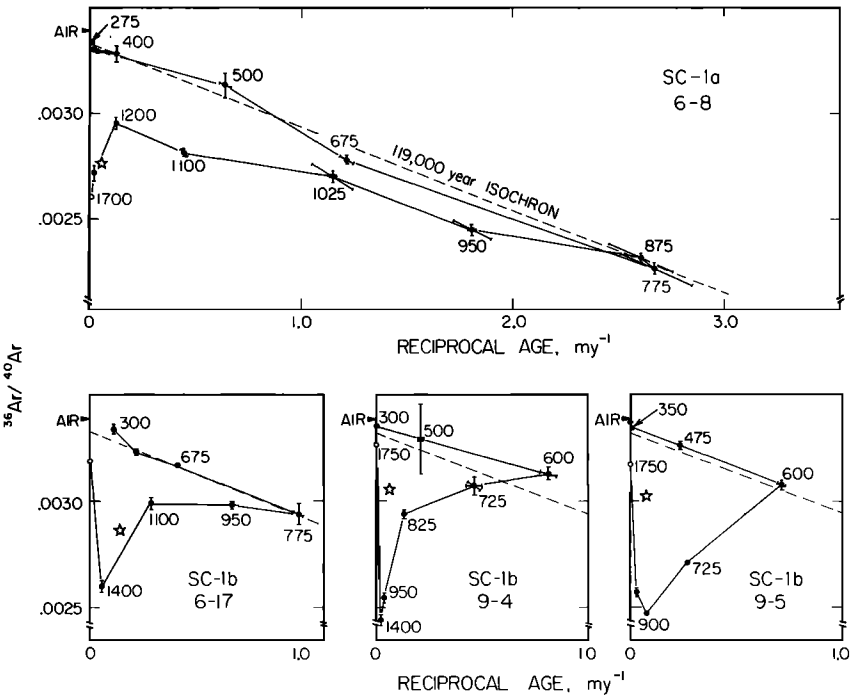

Fig. 3. Three-isotope diagrams for analyses of granodiorite xenoliths from site SC-1. Ar compositions range from near AIR on the ordinate (at low temperatures) along lines yielding a low age on the abscissa ($^{39}Ar/^{40}Ar$ normalized to units of reciprocal age); at higher temperatures they return to the ordinate along complicated trajectories. We interpret these patterns to show release of Ar of single trapped and K-derived compositions at low temperatures and the additional release of $^{40}Ar_0$* at high temperatures. The top diagram shows Ar compositions for xenolith SC-1a (sample 6-8). The 119,000-year line fit to the first eight compositions is probably an isochron. The bottom row shows compositions from three replicates of a second xenolith, SC-1b. The dashed line is the isochron from sample 6-8, included for reference. Only in the first three or four steps was Ar released free of $^{40}Ar_0$*. At higher temperatures Ar compositions are clearly affected by $^{40}Ar_0$* because they move progressively nearer the origin. Stars show total compositions. Open circles in this and subsequent figures denote uncertain compositions with large error bars. Temperatures (°C) are shown for selected steps.

Because fewer steps were free of $^{40}Ar_0$* than for sample 6-8, isochrons for the second xenolith were less precise. Nevertheless, at the 2σ level all four ages overlapped, and ages for samples 6-17 and 9-5 (Table 2) were within 1σ of 119,000 years, the age from sample 6-8. Only three steps for 9-4 appeared to be free of $^{40}Ar_0$*, and these were of low analytic precision.

The mean age calculated by weighting all four individual isochron ages by their respective variances was 117,000 ± 7000 years, not including the systematic 3.4% uncertainty of the monitor age.

5.2. *Xenolith Samples from Site SC-23*

Five samples of a single granodiorite xenolith from SC-23 were analyzed. Three of these (9-1, 9-2 and 6-25) were whole pieces of xenolith. Sample 6-16 was cut from a 2-cm K-feldspar phenocryst, and sample 9-6 consisted of etched feldspar grains picked from the crushed xenolith. Only 9-6 was wrapped in foil. Average abundances of K and Ca inferred for the xenolith samples (exclusive of the phenocryst) were 4.3 and 4.4%, respectively. Stepwise data for the five analyses are summarized in Table 3*c*; three-isotope diagrams are given in Figure 4.

Four of the five analyses were similar to those for the two xenoliths from site SC-1. Total ages of 2.6–5.1 m.y. indicated a comparable level of degassing in the lava. Composition trajectories for these four analyses were similar to those for the site SC-1 xenoliths (Figure 3). Maximum ages for the high-temperature steps were as high as 12 m.y. The low-temperature extractions defined lines giving ages of 104,000-161,000 years. ^{40}Ar for these steps was as much as 20% radiogenic.

Five extractions of Ar from xenolith sample 9-1, representing over half the ^{39}Ar released, appeared to be free of $^{40}Ar_0$* and were used to define an isochron for the age of eruption of the host lava (Figure 4). This isochron intercepted the ordinate within 1σ of "AIR" and indicated an age of 125,000 ± 23,000 years. One of the five compositions (600°C) plotted distinctly below the fitted line.

Compositions of Ar released from sample 9-2 in four steps at low temperatures clustered around only two values. Subsequent steps obviously released $^{40}Ar_0$*. A line fit to the low-temperature steps passed through the ordinate within 1σ of "AIR" and specified an age of eruption of 104,000 ± 37,000 years. As for 9-1, over half the total ^{39}Ar was released during these steps. However, without a trend of compositions it cannot be determined whether the 900°C step was free of $^{40}Ar_0$*, so the isochron age may be only an upper limit to the age of eruption.

Ar released from sample 6-25 in eight steps at temperatures at or below ~1025°C did define a linear array of compositions. The analysis of sample 6-25 together with sample 6-8 provides our best supporting evidence for the model of *Gillespie et al.* [1982]. A line fit to these points passed through the ordinate at $^{36}Ar/^{40}Ar$ = 0.00333 ± 0.00003, indicating an Ar_t richer in ^{40}Ar than atmospheric

TABLE 3c. Granodiorite Xenolith From Site SC-23

T, °C	^{40}Ar cm^3 STP g^{-1} × 10^8	^{40}Ar(Blank) cm^3 STP g^{-1} × 10^8	$^{39}Ar/^{40}Ar$ × 10^4	$^{36}Ar/^{40}Ar$ × 10^5	F_{39}	Model Age, m.y.
			Sample 9-1			
400*	13.	0.24	63 ± 0	340 ± 1	0.06	−0.1 ± 0.1
500*	7.8	0.24	162 ± 1	334 ± 1	0.15	0.18 ± 0.05
600*	2.7	0.24	615 ± 2	320 ± 3	0.27	0.19 ± 0.03
725*	0.72	0.24	3020 ± 18	281 ± 9	0.38	0.12 ± 0.02
900*	1.0	0.24	2536 ± 10	284 ± 6	0.53	0.13 ± 0.01
1000	3.0	0.24	378 ± 3	297 ± 3	0.61	0.69 ± 0.05
1400	28.0	3.9	205 ± 1	140 ± 1	0.98	6.13 ± 0.04
1750	21.0	13.0	37 ± 5	279 ± 16	1.00	9.9 ± 3.0
			Sample 9-2			
300*	3.1	0.97	22 ± 1	336 ± 6	0.002	0.7 ± 0.1
600*	35.	0.97	94 ± 1	327 ± 2	0.12	0.7 ± 1.6
725*	17.	0.97	401 ± 2	330 ± 2	0.36	0.13 ± 0.1
900*	2.7	0.97	2700 ± 29	291 ± 10	0.53	0.11 ± 0.02
~1100	22.	0.97	246 ± 1	158 ± 1	0.73	4.6 ± 0.0
1400	61.	6.7	134 ± 1	83 ± 16	1.00	12.0 ± 0.7
1750	48.	29.	1 ± 5	336 ± 18	1.00	· · ·
			Sample 6-25			
300*	12.	0.36	63 ± 1	332 ± 1	0.03	0.67 ± 0.15
500*	30.	0.36	104 ± 1	332 ± 1	0.16	0.37 ± 0.09
675*	14.	0.36	213 ± 1	325 ± 1	0.28	0.41 ± 0.04
675*	5.4	0.36	101 ± 1	332 ± 4	0.30	0.39 ± 0.25
775*	2.7	0.36	821 ± 3	322 ± 5	0.38	0.13 ± 0.04
875*	1.6	0.36	1482 ± 16	306 ± 8	0.46	0.14 ± 0.03
950*	1.1	0.36	1976 ± 10	298 ± 8	0.51	0.13 ± 0.03
1025*	0.67	0.36	3112 ± 20	278 ± 17	0.55	0.13 ± 0.04
1075	0.64	0.36	2241 ± 67	267 ± 24	0.58	0.20 ± 0.07
1200	62.	4.1	172 ± 1	114 ± 1	0.99	8.4 ± 0.0
1400	47.	40.	22 ± 1	316 ± 72	1.00	· · ·
			Sample 6-16. K-feldspar from granodiorite xenolith			
300*	5.8	0.32	23 ± 0	324 ± 1	0.003	4.0 ± 0.4
500*	4.4	0.32	131 ± 1	325 ± 1	0.02	0.67 ± 0.07
775*	4.3	0.32	760 ± 1	304 ± 3	0.08	0.29 ± 0.02
950*	1.2	0.32	2630 ± 19	267 ± 6	0.13	0.17 ± 0.02
1075*	1.2	0.32	2602 ± 13	259 ± 8	0.19	0.20 ± 0.02
1225	2.8	0.32	1111 ± 13	265 ± 7	0.25	0.4 ± 0.0
1300	46.	0.41	303 ± 0	189 ± 1	0.56	3.2 ± 0.0
1500	97.	2.5	190 ± 1	75 ± 1	0.96	8.9 ± 0.1
1525	24.	13.	164 ± 3	80 ± 15	1.00	10.1 ± 1.0
1750	41.	35.	21 ± 2	358 ± 68	1.00	· · ·
			Sample 9-6. Etched microcline from granodiorite xenolith			
350	29.	0.09	5 ± 0	338 ± 1	0.01	0.8 ± 0.9
425	7.4	0.09	275 ± 1	315 ± 2	0.07	0.5 ± 0.0
600	4.1	0.09	896 ± 3	235 ± 2	0.18	0.7 ± 0.0
750	6.2	0.09	403 ± 1	107 ± 1	0.26	3.6 ± 0.0
900	110.	0.09	51 ± 0	16 ± 3	0.43	39.7 ± 0.5
1100	810.	0.09	21 ± 0	6 ± 0	0.95	98.7 ± 0.2
1300	81.	9.4	18 ± 0	−8 ± 2†	1.00	116.1 ± 1.9
1600	28.	19.	16 ± 1	87 ± 22	1.00	94.4 ± 5.3

*Steps used to find isochrons.
†Negative value resulted from subtraction of nominal blank, which was excessive in this instance. Model age is essentially unaffected.

Ar. The regression line indicated an age of 117,000 ± 11,000 years, in agreement with the age of eruption of 117,000 ± 7000 years found from xenoliths from site SC-1 and also with the isochron ages from samples 9-1 and 9-2. Over half of the ^{39}Ar was released in these steps. Because of the large number of colinear steps defining the regression line and the good distribution of compositions, sample 6-25 gave the best isochron for site SC-23.

Sample 6-16 was part of a single K-feldspar phenocryst from xenolith SC-23. The first four or five steps appeared to be free of $^{40}Ar_0$* and clustered around three compositions which defined a slightly concave pattern. The first was virtually on the ordinate and showed an Ar_i obviously enriched in ^{40}Ar compared to "AIR." The regression line fit to the five low-temperature compositions gave an age of 161,000 ± 24,000 years, considerably greater than the other isochron ages. Only 19% of the total ^{39}Ar was released in the steps defining the isochron.

The weighted mean age of the four isochrons for site SC-23 was 123,000 ± 9000 years. This age overlapped the mean age of 117,000 ± 7000 years for isochrons for site SC-1.

The trajectory for the fifth analysis (sample 9-6) resembled those of the other four at high temperatures, but the linear trend of compositions toward a young K-derived Ar was not

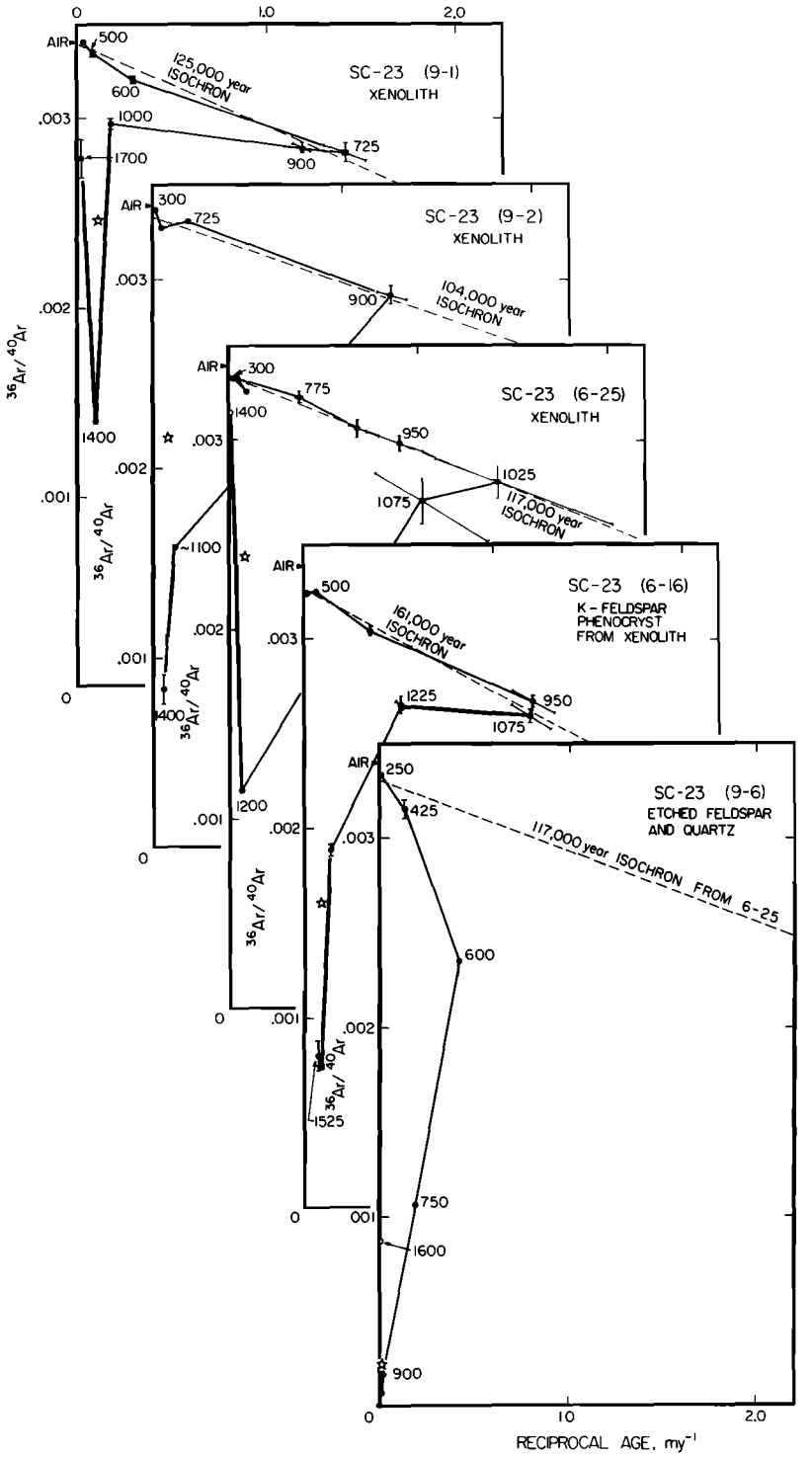

Fig. 4. Three-isotope diagrams for analyses of granitic xenolith samples from site SC-23. Ar released at low temperatures clearly showed the tendency to plot along a line between a well-defined Ar_r on the ordinate and a young K-derived $^{39}Ar/^{40}Ar$ (proportional to reciprocal age) on the abscissa. All samples appeared to release $^{40}Ar_0$* at temperatures above 1050°C. Sample 9-6 (etched in HF) alone released $^{40}Ar_0$* at such low temperatures that it clearly failed to define an isochron. Stars show total compositions. Temperatures (°C) are shown for selected steps.

present. The total age, 65 m.y., was more than a factor of 10 greater than the total ages of the other samples, so that the sample appeared to be poorly degassed. This probably resulted from the removal during etching in HF of the parts of the sample that were highly degassed in the lava. Thus sample 9-6 may show the trajectory associated with the retentive reservoirs of Ar alone. Ar released from 9-6 at ~1300°C gave an apparent age of 116 m.y., which is thus a lower limit to the age of the Spook pluton from which the xenoliths appear to have been derived.

5.3. *Xenolith Samples from Sites SC-115 and SC-118*

Site SC-115 was the same outcrop sampled by *Dalrymple* [1964*a*] for K/Ar dating of the basalt underlying the glacial

TABLE 3*d*. Granodiorite Xenoliths From Sites SC-118 and SC-115

T, °C	^{40}Ar cm^3 STP g^{-1} × 10^8	^{40}Ar(Blank) cm^3 STP g^{-1} × 10^8	$^{39}Ar/^{40}Ar$ × 10^4	$^{36}Ar/^{40}Ar$ × 10^5	F_{39}	Model Age, m.y.
			Sample 7-63 (SC-118)			
350	48.	0.95	7 ± 0	334 ± 1	0.03	3.5 ± 1.2
500	6.8	0.95	142 ± 1	337 ± 3	0.09	0.07 ± 0.13
600*	...	...	...	...	...	...
700	18.	0.95	106 ± 0	331 ± 1	0.24	0.37 ± 0.08
700	1.5	0.95	570 ± 5	300 ± 40	0.26	0.37 ± 0.38
900	2.8	0.95	599 ± 5	306 ± 13	0.35	0.30 ± 0.12
1000	3.1	0.95	753 ± 3	218 ± 11	0.48	0.88 ± 0.08
1200	41.	1.4	146 ± 1	67 ± 1	0.94	10.2 ± 0.1
1700	15.	7.9	102 ± 1	142 ± 7	1.00	10.6 ± 0.4
			Sample 7-82 (SC-115)			
275	9.	0.36	3 ± 0	338 ± 1	0.00	...
350	4.8	0.36	21 ± 0	330 ± 4	0.01	2.3 ± 1.0
425	2.3	0.36	316 ± 1	279 ± 4	0.04	1.0 ± 0.1
500	1.1	0.36	1348 ± 3	250 ± 8	0.10	0.36 ± 0.03
600	1.3	0.36	2183 ± 131	254 ± 15	0.21	0.21 ± 0.04
725	1.6	0.77	2684 ± 11	237 ± 13	0.33	0.21 ± 0.03
850	0.86	0.36	2720 ± 11	213 ± 11	0.41	0.25 ± 0.02
~1000	2.6	0.36	968 ± 2	122 ± 3	0.53	1.24 ± 0.02
1100	66.	0.46	110 ± 11	39 ± 9	0.94	14.9 ± 0.5
1750	32.	36.	...	...	1.00	...

Extraction temperatures are given in the first column. The second column shows the total ^{40}Ar released in each step, including blank ^{40}Ar (third column). Blank levels of ^{40}Ar are generally repeatable to ±50% (2σ). In a few cases uncertainties were ±25%. Ratios of ^{39}Ar and ^{36}Ar to ^{40}Ar (after all corrections, including removal of the blank Ar) are shown in columns four and five. Column six gives the cumulative fraction of ^{39}Ar (F_{39}) released up to and including the indicated step, and the final column shows the age indicated by the Ar compositions in columns four and five. The apparent ages were calculated according to the equation and proportionality factors given in Table 1. Ar_t was assumed to have atmospheric composition ($(^{36}Ar/^{40}Ar)_t$ = 0.003384). Ar from foil wrappings has been subtracted. Uncertainties are 2σ.

*Step lost.

moraine II (Figure 1). Site SC-118 was a second smaller outcrop of basalt under the same moraine. One granitic xenolith from each site was analyzed. Data for each step are summarized in Table 3*d*; three-isotope diagrams are shown in Figure 5.

Xenolith sample 7-63 from SC-118 had a total age of only 5.7 m.y., so it had been degassed to a level similar to those of xenoliths from sites SC-1 and SC-23. Despite this, the composition trajectory resembled that of the etched sample 9-6, and no isochron was defined.

Xenolith sample 7-82 from SC-115 had a total age of 6.8 m.y. The complicated trajectory proceeded from a composition near "AIR" at ~275°C to define a strongly concave pattern culminating at 725°C in a composition for which the ^{40}Ar was as much as 30% radiogenic. Subsequent steps appear to have released $^{40}Ar_0$* and plotted increasingly close to the origin. This pattern could indicate multiple Ar_t components released at low temperatures, recoil redistribution, or some other effect. It cannot be unambiguously interpreted, and we do not use it to define an isochron.

6. DISCUSSION

Ten ^{40}Ar-^{39}Ar analyses of partially degassed granitic xenoliths from three different sites in the basalt flows of Sawmill Canyon gave total ages ranging from 0.9 to 6.8 m.y. These ages are much greater than the K/Ar age of 53,000 ± 88,000 (2σ) years reported for the same basalt flow by *Dalrymple et al.* [1982]; however, they are consistent with the K/Ar age of 2.0 ± 0.1 m.y. reported for a granitic xenolith from that flow by *Dalrymple* [1964*b*]. The high total age for the xenoliths must be due to the presence of various amounts of $^{40}Ar_0$* undegassed upon heating in the basaltic magma. If the xenoliths first crystallized and closed to Ar diffusion in the Cretaceous Period, then degassing was at least 90% complete.

The stepwise ^{40}Ar-^{39}Ar analyses revealed consistent patterns of isotopic composition variation similar to those described by *Gillespie et al.* [1983] for similar xenoliths from a much older Pleistocene basalt flow. These complicated patterns differ from those for basalt samples by the presence of large amounts of $^{40}Ar_0$* in the high-temperature extractions. While overall these observed patterns cannot result from mixing between only one trapped and only one K-derived Ar, at least for some samples it appears that such binary mixing can describe the isotopic variation of Ar released at temperatures below ~950°C. At higher temperatures some Ar appears to be extracted from reservoirs at Ar_t as well as of the second, ancient K-derived Ar.

6.1. *Isochron Ages from the Granitic Xenoliths*

Lines fit in $^{36}Ar/^{40}Ar$ versus $^{39}Ar/^{40}Ar$ diagrams to linear arrays of compositions of Ar could well be isochrons giving the age of eruption of the host lava containing the xenoliths, as long as the extractions were at temperatures too low to release $^{40}Ar_0$* or a second Ar_t. We interpreted at least two of these regression lines as isochrons (6-8 and 6-25). These two isochrons gave a mean age (weighted by the variance) of 118,000 ± 6000 years. Ages for six other analyses ranged from 84,000 to 161,000 years and clustered about 119,000 years (Figure 6). The weighted mean age for these six analyses, 122,000 ± 10,000 years, was not significantly different from the age for the two best analyses. However,

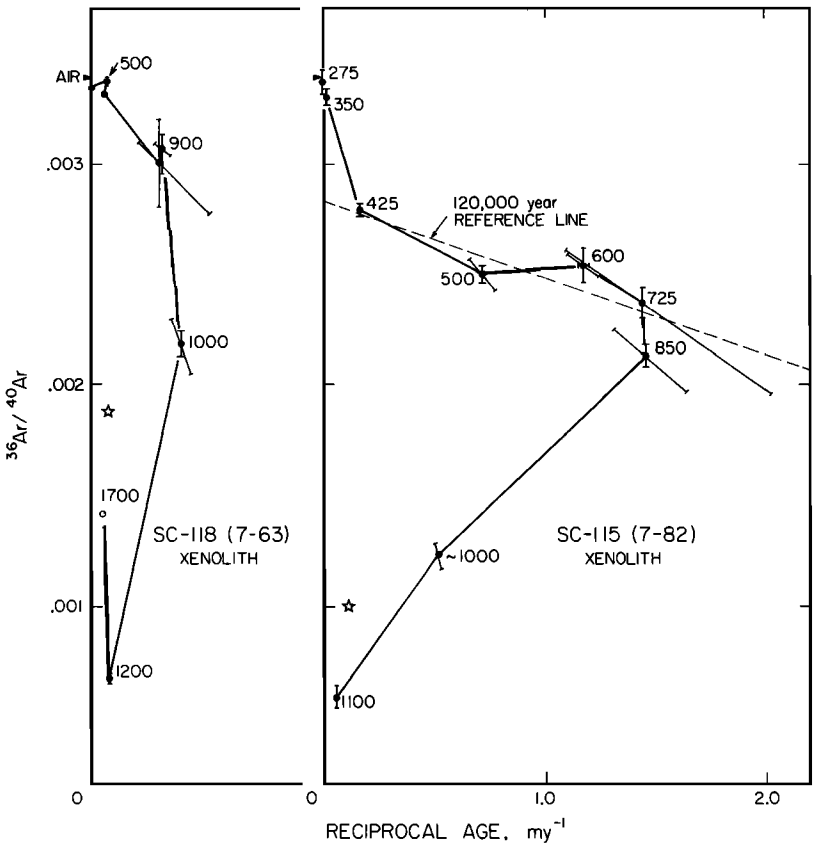

Fig. 5. Three-isotope diagrams for analyses of xenoliths from sites SC-118 and SC-115 from a basalt outcrop directly beneath moraine II. Ar compositions failed to define simple linear patterns for either xenolith. Temperatures (°C) are shown for selected steps.

two of the six samples (6-16 and 9-4) gave ages more than 2σ from the mean age for all samples. That these ages were so deviant probably indicates that the isotopic variations for these two samples should not be interpreted to define isochrons, but this could not be determined a priori. We therefore accept the weighted mean age from all the isochrons, 119,000 ± 7000 years (including systematic uncertainties), to be the age of eruption of the host basalt. The precision of this age, and of the best of the individual determinations, is comparable to the precision of conventional K/Ar analysis of ideal samples such as sanidine crystals of the same age [cf. *Bailey et al.*, 1976].

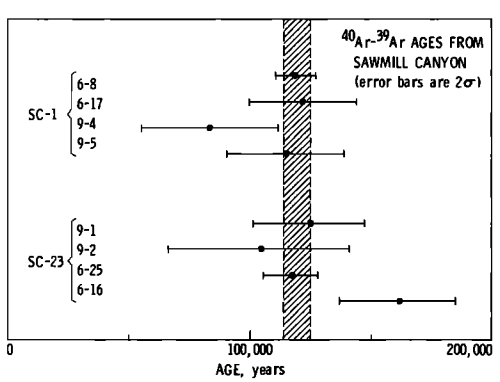

Fig. 6. Isochron ages for granitic xenolith samples from sites SC-1 and SC-23. Site and sample are shown to left. Ages are stacked above the time line. Shading shows the 95% confidence window for the mean age of all analyses, 119,000 ± 7000 years.

The most obvious source of error in the isochron ages was the unrecognized presence of $^{40}Ar_0$* in the low-temperature extractions. The effect of $^{40}Ar_0$* is a monotonic rise in the apparent age calculated for each step in the analysis. This rise can be seen in Figure 7, which contrasts age spectra for xenolith samples 6-8 and 6-16. $^{40}Ar_0$* appears to have been first released from the sample 6-8 during the 950°C step, after half the ^{39}Ar had already been extracted. Sample 6-16 showed the same increase in apparent age at similar extraction temperatures. However, far less ^{39}Ar was released without $^{40}Ar_0$* and it is not clear which step was the first affected. Thus, it is possible that the regression line for sample 6-16 was fit to affected compositions. This would be consistent with the high age for the sample.

6.2. *Trapped Argon*

The unrecognized presence of $^{40}Ar_0$* in the low-temperature extractions could not account for more than a few thousand years in the apparently high eruption age for sample 6-16, and does not explain the low age for sample 9-4. A second source of error in the isochron ages is suggested by the variable composition of Ar_t found for the different xenolith samples. Values of $(^{36}Ar/^{40}Ar)_t$ in Table 2 ranged from 0.00325 to 0.00337. Ar_t for three of the xenolith samples was distinctly enriched in ^{40}Ar compared to atmospheric Ar (difference $> 2\sigma$), and Ar_t for two other samples was probably enriched (difference $= 2\sigma$). Most convincing was sample 6-16, cut from a single K-feldspar phenocryst. Only 3.1×10^{-10} cm^3 STP/g of ^{36}Ar was extracted from the phenocryst in the first two steps (300°C and 500°C), com-

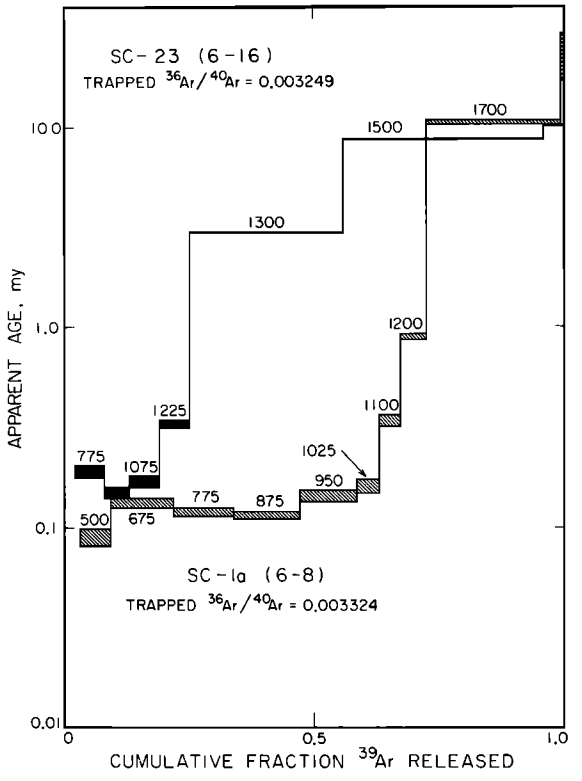

Fig. 7. Age spectra for granodiorite xenolith 6-8 from site SC-1a and for K-feldspar phenocryst 6-16 from a xenolith from site SC-23. Apparent ages have been calculated assuming a single composition of Ar_t specified by a line fit to compositions free of $^{40}Ar_0$* (Table 2), instead of assuming an Ar_t of atmospheric composition as in Table 3. There is an increase in apparent age as $^{40}Ar_0$* is released at high temperatures from retentive reservoirs. About half of the ^{39}Ar from 6-8 was released in low-temperature steps defining a plateau at the age of degassing or eruption of the host basalt. A much smaller fraction of ^{39}Ar was released from 6-16 in comparable low-age steps. The age spectrum for sample 6-25 (not shown) is in excellent agreement with the one for 6-8. Error bars are $\pm 1\sigma$.

pared to 1.4×10^{-9} cm^3 STP/g for adjacent xenolith sample 6-25. Perhaps the lower value of $(^{36}Ar/^{40}Ar)_t$ for the phenocryst was due to smaller amounts of atmospheric Ar adhered to the reduced surface area of the coarsely fractured phenocryst, compared to the aggregate of small grains in the rest of the xenolith. This explanation supposes two different trapped components: the adhered atmospheric Ar and an ^{40}Ar-rich component which must have been emplaced during cooling of the lava flow.

What then was the origin of this ^{40}Ar-rich trapped component? If our interpretive model is correct, upon heating in the magma non-retentive reservoirs should have been depleted not only of $^{40}Ar_0$* but also of Ar_t. Yet large amounts of Ar_t were extracted from samples in low-temperature steps free of $^{40}Ar_0$*. The enrichment in ^{40}Ar appears to rule out adhered atmospheric Ar as the source of this Ar_t, unless it was strongly fractionated. Another source could be Ar dissolved in the basaltic magma which diffused into the xenolith during cooling and after degassing of the $^{40}Ar_0$*. This process has been deduced by *Harrison and McDougall* [1980, 1981] for plagioclase and hornblende at ~350°C. An obvious source of ^{40}Ar would have been ancient wallrocks and xenoliths degassed by the magma.

Ar_t composed of a mixture of back-diffused magmatic Ar and atmospheric Ar adhered to the sample after cooling could explain the concave low-temperature isotopic composition trajectories found for sample 9-1 (Figure 4) and perhaps for sample 7-82 (Figure 5), if the adhered Ar were completely extracted before the rest of the Ar_t. Such a mixture of trapped components would increase not only the apparent total age, but also the isochron age. Thus the low age for sample 9-4 is not readily explained by this mechanism. Protection against the effects of mixed components lies in analyzing several samples using many extraction steps so that real trends in composition can be identified.

The total ages found for our basalt samples were well in excess of the age of eruption determined from the isochrons for the granitic xenoliths. There is no evidence in the three-isotope diagrams that these high ages were due to $^{40}Ar_0$* released from undetected xenocrysts in the lava. However, they could be explained if Ar dissolved in the magma and later trapped in crystals had been enriched by ^{40}Ar* degassed from ancient country rock.

6.3. *Effects of ^{39}Ar Recoil*

Recoil loss or redistribution of ^{39}Ar is potentially a serious source of error in ^{40}Ar-^{39}Ar analysis [cf. *Turner and Cadogan*, 1974; *Huneke and Smith*, 1976]. Saddle shaped age spectra from partially degassed microcline crystals have been attributed to ^{39}Ar recoil [cf. *Berger*, 1975; *Berger and York*, 1979]. In three-isotope diagrams, comparable effects might lead to excessively low isochron ages, such as observed for sample 9-4, if the redistributed ^{39}Ar was degassed in the first few extraction steps. However, in our best analyses (6-8 and 6-25), the compositions for low-temperature steps were colinear and there was no indication of recoil effects for the granitic xenoliths. That this linearity is not spurious is suggested by the agreement of isochron ages found for xenoliths and host basalt reported by *Gillespie et al.* [1983].

The total ages of the two basalt samples 2-2 and 2-3 were decidedly greater than the age of eruption found from the granitic xenoliths. Total ages should not be affected by recoil redistribution of ^{39}Ar, as long as there was no loss of ^{39}Ar from the sample. However, the high ages could be explained by loss of ~75% of the ^{39}Ar by recoil. *Huneke and Villa* [1981] and *Villa et al.* [1983] have reported losses of up to 60% from five samples of very fine-grained inclusions in the Allende meteorite, and *Turner and Cadogan* [1974] and *Halliday* [1974] have reported losses of up to 45% from powdered basalt and clays, respectively. This large loss of ^{39}Ar would be reflected in low apparent values of K, but such were not found (Table 1).

6.4. *Effects of $^{40}K(n, p)^{40}Ar$*

Tetley et al. [1980] have shown most $^{40}K(n, p)^{40}Ar$ is due to thermal rather than fast neutrons. They point out that the ratio of thermal neutrons to fast neutrons varies spatially and temporally for a given reactor. For example, the flux of the HIFAR reactor varies by a factor of <0.5 with position of the monitor in the reactor. The thermal neutron flux of the Herald reactor [*Turner*, 1971*b*] varies by a factor of <2.5 with time. Thus the pro forma correction we applied for $^{40}Ar_K$, $(^{40}Ar/^{39}Ar)_K = (5.9 \pm 0.4) \times 10^{-3}$ [*Dalrymple and Lanphere*, 1971], may have been in error by much more than the indicated uncertainty.

The effect of uncorrected $^{40}Ar_K$ is to increase the apparent age. The trajectory of compositions in the three-isotope

diagram is steepened, but the linearity of compositions is undisturbed. We found that the maximum $^{40}Ar_K/^{40}Ar^*$ was about 1% for xenolith 6-8. For the young ages of interest in this study, the error in age resulting from $^{40}Ar_K$ is linear with this factor. If the $(^{40}Ar/^{39}Ar)_K$ correction factor we used was accurate to within a factor of 3, maximum bias to the apparent age of an individual step was less than 3% for sample 6-8.

6.5. *Diffusive Loss of $^{40}Ar^*$ at Very Low Temperatures*

Diffusive loss from microcline of new $^{40}Ar^*$ created after eruption is probably an unimportant source of error. *Khutsaidze* [1962] measured less than 2% loss in eight hours at temperatures below 400°C. *Harrison and McDougall* [1982] found that microcline is effectively closed to Ar diffusion at temperatures below 100°C. Reported loss of Ar from microcline [*Wasserburg et al.*, 1956] could have taken place at elevated temperatures before exposure at the earth's surface. The xenoliths we analyzed have probably not been heated above 50°C since cooling of the host lava, and the effects of any minor diffusive loss of $^{40}Ar^*$ which did occur after cooling of the lava are probably confined to the first extraction step.

6.6. *Geologic Significance*

The lava flow dated in this study is intercalated between glacial moraines of two different ages. One motivation for dating the flow was to establish precise age limits for those glaciations. At the same time, previous estimates of the ages of the glaciations could be used to reject grossly inaccurate dates for the flow. The glacial history of Sawmill Canyon has been repeatedly studied [*Knopf*, 1918; *Moore*, 1963; *Dalrymple*, 1964*a*; *Burke and Birkeland*, 1979; *Gillespie*, 1982]. In each study, the glacial deposits were correlated to better understood sequences of tills in other canyons of the Sierra Nevada and elsewhere, using relative dating techniques which depend on subjective and semiquantitative comparison of the extent of rock weathering and soil development [cf. *Blackwelder*, 1931; *Sharp and Birman*, 1963; *Burke and Birkeland*, 1979]. All workers agreed that moraine II (overlying the lava flow, Figure 1) was built during the Wisconsin glaciation, which from $\delta^{18}O$ variations in marine sediments [*Shackleton and Opdyke*, 1976] occurred between ~13,000 and ~75,000 years ago (*Smith* [1979] suggests that the onset of glaciation in the Sierra Nevada may have been as early as ~90,000 years ago). *Moore* [1963] and *Burke and Birkeland* [1979] assigned moraine II to the Tioga glaciation, ~13,000 to ~32,000 years ago, and moraine I to the Tahoe glaciation, ~64,000 to ~75,000 years ago (age estimates follow *Shackleton and Opdyke* [1976]). The Tioga and Tahoe advances are names local to the Sierra Nevada, and probably correspond respectively to late and early Wisconsin glaciations. *Dalrymple* [1964*a*] and *Gillespie* [1982] felt that moraine I was pre-Tahoe (probably more than ~128,000 years old). All agreed that moraine I was significantly younger than the Sherwin glaciation (local name), which preceded the eruption of the Bishop Tuff 730,000 years ago [*Dalrymple et al.*, 1965; *Sharp*, 1968]. Thus the high total ages of the granitic xenoliths could not correspond to the age of the Sawmill Canyon lava flow, and had to result from incomplete degassing of $^{40}Ar_0^*$. The isochron ages for the xenoliths, and even the total ages for the basalts, were all geologically possible in at least one of the two interpretations of the glacial history.

The age of eruption determined from the granitic xenoliths, 119,000 ± 7,000 years, must be an upper limit for the age of moraine II and a lower limit for moraine I. This supports the glacial history of *Dalrymple* [1964*a*] and *Gillespie* [1982], since moraine I clearly must be pre-Tahoe or pre-Wisconsin.

7. SUMMARY AND CONCLUSIONS

We have analyzed eleven samples from five partially degassed Mesozoic granitic xenoliths and two late Pleistocene host basalt samples from Sawmill Canyon using stepwise ^{40}Ar-^{39}Ar dating techniques. The basalt analyses did not yield a reliable age of eruption because the isotopic compositions did not define isochrons, and the total ages appeared to be excessive. We attributed these high apparent ages to the presence of a trapped Ar enriched in ^{40}Ar, perhaps through degassing of ancient wallrocks and xenoliths by the rising magma.

Analyzing granitic xenoliths appeared to give much better results than analyzing the host basalt. For some analyses, more than half the ^{39}Ar was released in low-temperature steps free of the $^{40}Ar^*$ that was retained in the xenoliths after heating in the magma ($^{40}Ar_0^*$). Subsequent steps at higher temperatures released large quantities of $^{40}Ar_0^*$ sufficient to raise the apparent total ages an order of magnitude or more above the age of eruption. Lines fit to $^{36}Ar/^{40}Ar$ versus $^{39}Ar/^{40}Ar$ diagrams for the Ar compositions unaffected by the $^{40}Ar_0^*$ were, for two samples, interpreted to give the age of degassing of the xenoliths, and hence the age of eruption of the host basalt. Regression lines were defined for six other analyses. Although interpretation of these lines as isochrons was less confident, they yielded ages generally compatible with the ages given by the two best analyses. Together, the eight analyses gave a weighted mean age of 119,000 ± 7,000 years, which we take to be the age of the eruption.

Isochrons for the xenoliths indicated trapped Ar may have been enriched in ^{40}Ar compared to atmospheric Ar. ^{40}Ar-^{39}Ar is potentially more accurate than conventional K/Ar analysis because such effects can be recognized and corrected. Because of the simple linear character of some of the isotope composition trajectories for Ar extracted below ~950°C, we feel there is no evidence for recoil or other complications in seven of the analyses. That the eruption is three orders of magnitude younger than the original crystallization of the xenoliths emphasizes the exceptional ability of high-resolution stepwise heating to separately release Ar from different reservoirs or sites.

We conclude that the age of eruption of young basalt flows can be reliably determined by ^{40}Ar-^{39}Ar analyses of ancient granitic xenoliths only partially degassed in the lava. This approach may be preferable to dating the lavas themselves. The high precision of the isochron ages from the partially degassed granitic xenoliths is comparable to the precision of K/Ar ages from sanidine crystals of equivalent age. The precise age of 119,000 ± 7000 years found from ^{40}Ar-^{39}Ar analysis of the granitic xenoliths provides a lower limit to the age of glacial advance I and an upper limit to advance II in Sawmill Canyon. *Dalrymple* [1964*a*] considered advance II to be of early Wisconsin age and advance I to be from an earlier glaciation. The new age of eruption is consistent with that interpretation.

Acknowledgments. We thank Glenn Berger and Mark Harrison for their thorough and thoughtful formal reviews. We are grateful to Art Chodos of Caltech for electron microprobe analyses and to Kathleen Baird of JPL for X-ray diffraction analyses. This research was supported by National Science Foundation grants EAR 78-01717 and EAR 79-19997 and by the Jet Propulsion Laboratory, California Institute of Technology, under contract to the National Aeronautics and Space Administration. Contribution 3629 (392) of the Division of Geological and Planetary Sciences, California Institute of Technology.

REFERENCES

Bailey, R. A., G. B. Dalrymple, and M. A. Lanphere, Volcanism, structure, and geochronology of the Long Valley Caldera, Mono County, California, *J. Geophys. Res., 81,* 725–744, 1976.

Berger, G. W., ^{40}Ar/^{39}Ar step heating of thermally overprinted biotite, hornblende and potassium feldspar from Eldora, Colorado, *Earth Planet. Sci. Lett., 26,* 387–408, 1975.

Berger, G. W., and D. York, ^{40}Ar-^{39}Ar dating of multicomponent magnetizations in the Archaean Shelby Lake granite, northwestern Ontario, *Can. J. Earth Sci., 16,* 1933–1941, 1979.

Blackwelder, E., Pleistocene glaciation in the Sierra Nevada and Basin ranges, *Geol. Soc. Am. Bull., 42,* 865–922, 1931.

Burke, R. M., and P. W. Birkeland, Reevaluation of multiparameter relative dating techniques and their application to the glacial sequence along the eastern escarpment of the Sierra Nevada, California, *Quat. Res., 11,* 21–51, 1979.

Curry, R. R., *Glacial and Pleistocene History of the Mammoth Lakes Area, California—A Geologic Guidebook, Geol. Ser. Publ.,* vol. 11, 49 pp., University of Montana, Department of Geology, Missoula, Mont., 1971.

Dalrymple, G. B., Potassium-argon dates of three Pleistocene interglacial basalt flows from the Sierra Nevada, California, *Geol. Soc. Am. Bull., 75,* 753–758, 1964*a*.

Dalrymple, G. B., Argon retention in a granitic xenolith from a Pleistocene basalt, Sierra Nevada, California, *Nature, 201,* 282, 1964*b*.

Dalrymple, G. B., and M. A. Lanphere, ^{40}Ar/^{39}Ar technique of K-Ar dating: A comparison with the conventional technique, *Earth Planet. Sci. Lett., 12,* 300–308, 1971.

Dalrymple, G. B., A. Cox, and R. E. Doell, Potassium-argon age and paleomagnetism of the Bishop Tuff, California, *Geol. Soc. Am. Bull., 76,* 665–674, 1965.

Dalrymple, G. B., E. C. Alexander Jr., M. A. Lanphere, and G. P. Kraker, Irradiation of samples for ^{40}Ar/^{39}Ar dating using the Geological Survey TRIGA Reactor, *U.S. Geol. Surv. Prof. Pap., 1176,* 55 pp., 1981.

Dalrymple, G. B., R. M. Burke, and P. W. Birkeland, Note concerning K-Ar dating of a basalt flow from the Tahoe-Tioga interglaciation, Sawmill Canyon, southeastern Sierra Nevada, California, *Quat. Res., 17,* 120–122, 1982.

Gillespie, A. R., Quaternary glaciation and tectonism in the southeastern Sierra Nevada, Inyo County, California, Ph.D. thesis, 695 pp., Calif. Inst. of Technol., Pasadena, 1982.

Gillespie, A. R., J. C. Huneke, and G. J. Wasserburg, An assessment of ^{40}Ar-^{39}Ar dating of incompletely degassed xenoliths, *J. Geophys. Res., 87,* 9247–9257, 1982.

Gillespie, A. R, J. C. Huneke, and G. J. Wasserburg, Eruption age of a Pleistocene basalt from ^{40}Ar-^{39}Ar analysis of partially degassed xenoliths. *J. Geophys. Res., 88,* 4997–5008, 1983.

Hall, C. M., and D. York, K-Ar and ^{40}Ar/^{39}Ar age of the Laschamp geomagnetic polarity reversal, *Nature, 274,* 462–464, 1978.

Halliday, A. N., ^{40}Ar-^{39}Ar stepheating studies of clay concentrates from Irish orebodies, *Geochim. Cosmochim. Acta, 42,* 1851–1858, 1974.

Harrison, T. M., and I. McDougall, Investigations of an intrusive contact, northwest Nelson, New Zealand, II, Diffusion of radiogenic and excess ^{40}Ar in hornblende revealed by ^{40}Ar/^{39}Ar age spectrum analyses, *Geochim. Cosmochim. Acta, 44,* 2005–2020, 1980.

Harrison, T. M., and I. McDougall, Excess ^{40}Ar in metamorphic rocks for Broken Hill, New South Wales: Implications for ^{40}Ar/^{39}Ar age spectra and the thermal history of the region, *Earth Planet. Sci. Lett., 55,* 123–149, 1981.

Harrison, T. M., and I. McDougall, The thermal significance of potassium feldspar K-Ar ages inferred from ^{40}Ar/^{39}Ar age spectrum results. *Geochim. Cosmochim. Acta, 46,* 1811–1820, 1982.

Huneke, J. C., Diffusion artifacts in dating by stepwise thermal release of rare gases, *Earth Planet. Sci. Lett., 28,* 407–417, 1976.

Huneke, J. C., and S. P. Smith, The realities of recoil: ^{39}Ar recoil out of small grains and anomalous age patterns in ^{39}Ar-^{40}Ar dating, *Proc. Lunar Planet. Sci. Conf. 7th, 2,* 1987–2008, 1976.

Huneke, J. C., and I. M. Villa, ^{39}Ar loss during neutron irradiation and the aging of Allende inclusions (abstract), *Meteoritics, 16*(4), 329, 1981.

Jäger, E., E. E. Niggli, and H. Baethge, Two standard minerals, biotite and muscovite, for Rb-Sr and K-Ar age determinations, sample Bern 4B and Bern 4M from a gneiss from Brione, Valle Verzasca (Switzerland), *Schweiz. Mineral. Petrogr. Mitt., 43,* 465–470, 1963.

Jessberger, E. K., J. C. Huneke, F. A. Podosek, and G. J. Wasserburg, High resolution argon analysis of neutron-irradiated Apollo 16 rocks and separated minerals, *Proc. Lunar Planet. Sci. Conf. 5th, 2,* 1419–1449, 1974.

Kermack, K. A., and J. B. S. Haldane, Organic correlation and allometry, *Biometrika, 37,* 30–41, 1950.

Khutsaidze, A. L., Experimental investigation of diffusion of radiogenic argon in feldspars and micas, *Geochemistry, 11,* 1063–1068, 1962.

Knopf, A., A geologic reconnaissance of the Inyo Range and the eastern slope of the southeastern Sierra Nevada, California, with a section on the stratigraphy of the Inyo Range by Edwin Kirk, *U.S. Geol. Surv. Prof. Pap., 110,* 130 pp., 1918.

Lanphere, M. A., and G. B. Dalrymple, Identification of excess ^{40}Ar by the ^{40}Ar/^{39}Ar age spectrum technique, *Earth Planet. Sci. Lett., 32,* 141–148, 1976.

Merrihue, C. M., and G. Turner, Potassium-argon dating by activation with fast neutrons, *J. Geophys. Res., 71,* 2852–2857, 1966.

Moore, J. G., Geology of the Mount Pinchot quadrangle, southern Sierra Nevada, California, *U.S. Geol. Surv. Bull., 1130,* 152 pp., 1963.

Radicati di Brozolo, F., J. C. Huneke, D. A. Papanastassiou, and G. J. Wasserburg, ^{40}Ar-^{39}Ar and Rb-Sr age determinations in Quaternary volcanic rocks, *Earth Planet. Sci. Lett., 73,* 445–456, 1981.

Shackleton, N. J., and N. D. Opdyke, Oxygen-isotope and paleomagnetic stratigraphy of Pacific Core V28-239: Late Pliocene to latest Pleistocene, *Mem. Geol. Soc. Am., 145,* 449–464, 1976.

Sharp, R. P., Sherwin Till-Bishop Tuff relationship, Sierra Nevada, California, *Geol. Soc. Am. Bull., 79,* 351–364, 1968.

Sharp, R. P., and J. H. Birman, Additions to the classical sequence of Pleistocene glaciations, Sierra Nevada, California, *Geol. Soc. Am. Bull., 74,* 1079–1086, 1963.

Smith, G. I., Subsurface stratigraphy and geochemistry of late Quaternary evaporites, Searles Lake, California, *U.S. Geol. Surv. Prof. Pap., 1043,* 130 pp., 1979.

Steiger, R. H., and E. Jäger, Subcommission on Geochronology: Convention on the use of decay constants in geo- and cosmochronology, *Earth Planet. Sci. Lett., 36,* 359–362, 1977.

Tetley, N., I. McDougall, and H. R. Heydigger, Thermal neutron interferences in the ^{40}Ar/^{39}Ar dating technique, *J. Geophys. Res., 85,* 7201–7205, 1980.

Turner, G. Argon 40/Argon 39 dating of lunar rock samples, *Proc. Apollo 11 Lunar Sci. Conf., 2,* 1665–1684, 1970.

Turner, G., ^{40}Ar-^{39}Ar ages from the lunar maria, *Earth Planet. Sci. Lett., 11,* 169–191, 1971*a*.

Turner, G., Argon 40-argon 39 dating: The optimization of irradiation parameters, *Earth Planet. Sci. Lett., 10,* 227–234, 1971*b*.

Turner, G., and P. H. Cadogan, Possible effects of ^{39}Ar recoil in ^{40}Ar-^{39}Ar dating of lunar samples, *Proc. Lunar Planet. Conf. 5th, 2,* 1601–1615, 1974.

Villa, I. M., J. C. Huneke, and G. J. Wasserburg, ^{39}Ar recoil losses and presolar ages in Allende inclusions, *Earth Planet. Sci. Lett., 63,* 1–12, 1983.

Wasserburg, G. J., R. J. Hayden, and K. J. Jensen, A^{40}-K^{40} dating of igneous rocks and sediments, *Geochim. Cosmochim. Acta, 10,* 153–165, 1956.

Williamson, J. H., Least-squares fitting of a straight line, *Can. J. Phys., 46,* 1845–1847, 1968.

York, D., Topographic map of the Mt. Pinchot Quadrangle, Inyo Co., California, 15 minute series, U.S. Geol. Surv., Reston, Va., 1953.

York, D., Least-squares fitting of a straight line, *Can. J. Phys., 44,* 1079–1086, 1966.

A. R. Gillespie, Jet Propulsion Laboratory, Mail Station 183-501, 4800 Oak Grove Drive, Pasadena, CA 91109.

J. C. Huneke, Charles Evans and Associates, San Mateo, CA 94402.

G. J. Wasserburg, The Lunatic Asylum of the Charles Arms Laboratory, Division of Geological and Planetary Sciences, California Institute of Technology, Pasadena, CA 91125.

(Received March 25, 1983;
revised November 15, 1983;
accepted November 17, 1983.)